

# Multivariate phase space reconstruction by nearest neighbor embedding with different time delays

Sara P. Garcia\*

*Biomathematics Group, Instituto de Tecnologia Química e Biológica,  
Universidade Nova de Lisboa, Rua da Quinta Grande 6, 2780-156 Oeiras, Portugal*

Jonas S. Almeida

*Department of Biostatistics, Bioinformatics and Epidemiology,  
Medical University of South Carolina, 135 Cannon Street, Charleston, South Carolina 29425, USA*

(Dated: June 12, 2018)

A recently proposed nearest neighbor based selection of time delays for phase space reconstruction is extended to multivariate time series, with an iterative selection of variables and time delays. A case study of numerically generated solutions of the  $x$ - and  $z$  coordinates of the Lorenz system, and an application to heart rate and respiration data, are used for illustration.

(©2005 The American Physical Society, <http://link.aps.org/abstract/PRE/v72/e027205>)

PACS numbers: 05.45.Tp, 87.19.Hh

Phase space reconstruction by time delay embedding is at the center of most nonlinear time series analysis methods (see [1, 6] for an introduction). It is a primal goal as it ensures, under certain generic conditions, the reconstruction of a phase space equivalent to the original one, thus allowing a qualitative and quantitative analysis of the underlying dynamical system. The most commonly used embedding techniques are based on Takens embedding theorem [11], which only considers delay-coordinate maps built from a single observable, that is, a scalar time series [10, 11]. Even though the widespread use and paramount importance of this embedding theorem, it can be extremely difficult to reconstruct a phase space from a scalar time series when more than a couple degrees of freedom are active [5], which is the common scenario when analyzing biological systems, due to the complexity of their structures and complicated dynamics. The motivation for this study is the increasing interest in reverse-engineering biological systems directly from time series (see [12] for example), whose typical multivariate, finite and noisy nature renders it particularly important to develop efficient multivariate embedding schemes [4].

Generically consider a smooth deterministic dynamical system  $s(t) = f(s(t_0))$ , either in continuous or discrete time, whose trajectories are asymptotic to a compact  $d$ -dimensional manifold. By performing  $k$ -dimensional measurements on the system, where  $k = 1, \dots, d$ , it is possible to define a function  $\mathbf{x}_{(i)} = h[s(t = i \times \delta)]$  that relates the states of the dynamical system throughout time with a time series of measured points, where  $\mathbf{x}_{(i)} \in \mathbb{R}^k$ ,  $i = 1, \dots, n$ ;  $n$  is the total number of sampled points, and  $\delta$  is the sampling time. Phase space reconstruction by time delay embedding is a method of generating an  $m$ -

dimensional manifold, from the  $(n \times k)$  available measurements, that is equivalent to the original  $d$ -dimensional manifold. In the scalar scenario, that is, for  $k = 1$ , an  $m$ -dimensional embedding matrix of delay-coordinate column vectors can be defined from the initial time series  $\mathbf{x}_{(i)}$ , as  $\mathbf{X} = [\mathbf{x}_{(i)}, \mathbf{x}_{(i+\tau_1)}, \mathbf{x}_{(i+\tau_2)}, \dots, \mathbf{x}_{(i+\tau_{(m-1)})}]$ . Building such a matrix implies estimating two parameters: the time delay  $\tau$ , which is the time displacement between successive columns, and the embedding dimension  $m$ , which is the dimension, or number of columns, of the final embedding matrix. We have recently proposed [3] a nearest neighbor measure  $N$  for time delay embedding, solely based on topological and dynamical arguments documented by the data. This measure possesses the useful feature of retaining the inverse relationship with structure disclosure, meaning that it first decreases with  $\tau$ , and then returns to higher values when  $\tau$  is too long for dynamic coupling to be retained. When the time series is noise-free, such  $\tau$  value corresponds to the global minimum of  $N$  and an upper limit to an efficient selection of time delays, beyond which statistical independence reflects dynamic decoupling. Furthermore, it was shown [3] that using different time delays for consecutive embedding dimensions is more efficient than using the same  $\tau$  value for all dimensions, which has been the common approach to phase space reconstruction by time delay embedding. Hence, the  $N$  algorithm will output a vector of different time delays  $[\tau_1, \tau_2, \dots, \tau_{(m-1)}]$ , as incorporated in the definition of embedding matrix above. In this report we extend that nearest neighbor embedding with different time delays method to multivariate time series, that is, when  $1 < k < d$ , by selecting, at each iteration, the combination of variable, from the initial set of  $k$  variables, and time delay that first minimizes  $N$ . As before [3], the false nearest neighbors (F) algorithm proposed by Kennel *et al.* [7] is used to set the final embedding dimension. This algorithm considers the ratio of

---

\*Email address:spinto@itqb.unl.pt

Euclidean distances between each and every point and its nearest neighbor, first on a  $m$ -dimensional and then on a  $(m + 1)$ -dimensional space. If the ratio is greater than a given threshold, these points are referred to as false nearest neighbors, that is, points that appear to be nearest neighbors not because of the dynamics, but because the attractor is being viewed in an embedding space too small to unfold it. When the fraction of F as a function of the embedding dimension decreases to zero, the underlying attractor is unfolded and  $m$  can be optimally estimated.

The nearest neighbor embedding with different time delays algorithm for multivariate time series is detailed below. (i) Consider an initial multivariate time series  $\mathbf{x}_{[i \times k]}$ ,  $i = 1, \dots, n$ , of  $n$  measurements of  $k$  different dynamical variables. For each variable and for each  $\tau$  being tested, build a candidate embedding matrix  $\mathbf{T}$ :

for  $j$  from 1 to  $k$  {  
  for  $\tau$  from 1 to  $\frac{1}{10}n$  { define  $\mathbf{T} = [\mathbf{x}_{(i,1:k)}, \mathbf{x}_{(i+\tau,j)}]$  }  
}

(the upper limit for  $\tau$  is chosen arbitrarily). (ii) For each  $(k + 1)$ -dimensional point, that is, for each row in matrix  $\mathbf{T}$ , estimate its  $(k + 1)$ -dimensional nearest neighbor. Calculate the Euclidean distance between them  $d_{E1}$ . (iii) Consider both points one sampling unit ahead, still in  $(k + 1)$ -dimensions, and calculate the new Euclidean distance between them  $d_{E2}$ . (iv) Estimate the ratio  $d_{E2}/d_{E1}$  and save the number of distance ratios larger than 10. That fraction is what is referred to as  $N$  in the  $\tau$  selecting profiles ahead. The threshold value, though heuristically set, is justified by numerical studies [7] and has low parametric sensitivity. (v) From the profiles of  $N$  vs  $\tau$  for each of the  $k$  variables, select the combination of variable and time delay that first minimizes  $N$ . That should be the optimal variable  $j_1$  and time delay  $\tau_1$  selection for this first embedding cycle (that is, each iteration that adds another dimension to the candidate embedding matrix). (vi) Estimate the percentage of F and save that value as a function of the dimensionality of the candidate embedding matrix  $\mathbf{T}$ . (vii) Build a putative embedding matrix  $\mathbf{X} = [\mathbf{x}_{(i,1:k)}, \mathbf{x}_{(i+\tau_1,j_1)}]$ , where  $1 \leq j_1 \leq k$ . (viii) Again, for each variable and  $\tau$  being tested, build a candidate embedding matrix, now  $\mathbf{T} = [\mathbf{x}_{(i,1:k)}, \mathbf{x}_{(i+\tau_1,j_1)}, \mathbf{x}_{(i+\tau,j)}]$ . (ix) Repeat steps (ii) to (viii), considering that now points are  $(k + 2)$ - and more dimensional. (x) Stop this iterative procedure when the fraction of F [step (vi)] has dropped to 0. The outcome of running this procedure for as long as necessary to minimize F is the final  $m$ -dimensional embedding matrix:  $\mathbf{X} = [\mathbf{x}_{(i,1:k)}, \mathbf{x}_{(i+\tau_1,j_1)}, \mathbf{x}_{(i+\tau_2,j_2)}, \dots, \mathbf{x}_{(i+\tau_{(m-k)},j_{(m-k)})}]$ , where  $\tau \in \mathbb{N}$  and  $1 \leq j \leq k$ .

Two bivariate data sets will be used to illustrate the multivariate extension of the nearest neighbor embedding with different time delays. The first are the  $x$ - and  $z$  coordinates [ $L(X)$  and  $L(Z)$ , respectively] of the Lorenz system of differential equations [8]  $\dot{x} = \sigma(y - x)$ ,  $\dot{y} = x(\rho - z) - y$ ,  $\dot{z} = xy - \beta z$ , with parameters

$\sigma = 10, \rho = 28, \beta = 8/3$ . The equations were numerically integrated with a 4–5th order Runge-Kutta algorithm, sampled at  $\delta = 0.01$  intervals, and transients were removed. The second data set is composed by two physiological signals, the heart rate [ $P(H)$ ] and respiration [ $P(R)$ ] from a 49-year-old man diagnosed with sleep apnea, a potentially life-threatening disorder in which the subject stops breathing during sleep. The data was extracted from data set B of the 1991 *Santa Fe Time Series Prediction and Analysis Competition* [9]. The variables were digitized at 250 Hz and then sampled at 0.5 second intervals. The units of the  $P(H)$  measurements are beats per minute, while  $P(R)$  is provided in uncalibrated digitization units (see [9] for more detailed information on the data set and its pre-processing). When considering multivariate time series, normalization is a pivotal prerequisite to overcome scale shifts. Accordingly, we have non-parametrically normalized each variable separately to its empirical cumulative distribution, by first sorting all  $n$  values and then replacing them by their  $rank/n$ . Each data set, as used in the subsequent analysis, includes a total of 8000 points, part of which is plotted in Fig. 1. The section of data set B used in this report includes both a period of apnea and a period of intermittent apnea.

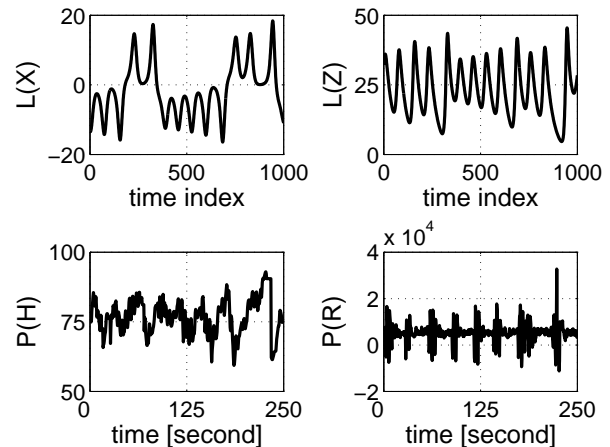


FIG. 1: Data sets. Upper panel: the  $x$  [ $L(X)$ , left] and  $z$  [ $L(Z)$ , right] coordinates of the Lorenz system. Lower panel: heart rate [ $P(H)$ , left] and respiration [ $P(R)$ , right] signals, in beats per minute and uncalibrated digitization units, respectively. In the subsequent analysis, each variable is normalized to its empirical cumulative distribution.

First, consider the case study of two coordinates of the Lorenz system. As this is a low-dimensional system, there is no obvious advantage in using multivariate time series to reconstruct the phase space. Therefore, this example is used only to illustrate the multivariate procedure for a well-described system, where the problems of noise and nonstationarity, typically encountered in biological data sets, are absent. The  $N$  profiles for

selecting  $\tau$  for the first embedding cycle are displayed in Fig. 2(a), where the thick line indicates the profile for  $L(X)$ , meaning that the candidate matrix being tested is  $[L(X)_{(i)}, L(Z)_{(i)}, L(X)_{(i+\tau)}]$ , and the thin line indicates the profile for  $L(Z)$ , meaning that the candidate matrix being tested is  $[L(X)_{(i)}, L(Z)_{(i)}, L(Z)_{(i+\tau)}]$ . The variable  $L(X)$  and the  $\tau$  value of its  $N$  profile first minimum  $\tau_1$  are the optimal combination that is selected from this first embedding cycle [Fig. 2(a), circle], which implies that the candidate embedding matrices that would be tested in a second embedding cycle would be  $[L(X)_{(i)}, L(Z)_{(i)}, L(X)_{(i+\tau_1)}, L(X)_{(i+\tau)}]$  and  $[L(X)_{(i)}, L(Z)_{(i)}, L(X)_{(i+\tau_1)}, L(Z)_{(i+\tau)}]$ . The rationale for using the first minimum was discussed in [3], where it was shown to be the most efficient choice. Displayed in Fig. 2(b) is the fraction of F as a function of  $m$  [7], from which can be concluded that the optimal embedding dimension is  $m = 3$ , and the final embedding matrix is then  $[L(X)_{(i)}, L(Z)_{(i)}, L(X)_{(i+\tau_1)}]$ .

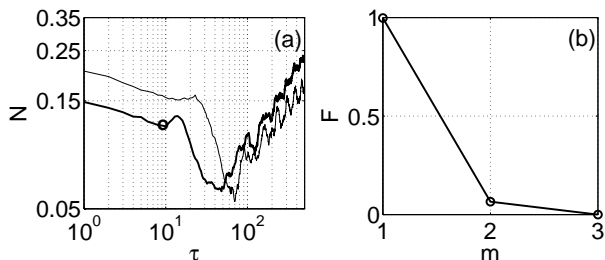


FIG. 2: (a) First embedding cycle profiles for  $\tau$  selection from  $N$ . The thick line indicates the profile for  $L(X)$  and the thin line the profile for  $L(Z)$ . A circle indicates the optimal combination of variable and time delay that is selected from this first cycle. The global minima of  $N$  corresponds to the onset of dynamic decoupling. (b) The fraction of F as a function of  $m$  for the embedding of the bivariate  $L(X)$  and  $L(Z)$  time series. See the text for a more comprehensive description.

Consider now the biological data set. Physiological systems are typically high-dimensional, nonstationary and contaminated by noise. We have taken no action to correct these problems, in the sense that we have used the data as given for the *Santa Fe Competition*. The  $\tau$  selecting profiles for the first, second, third and fourth embedding cycles are displayed in Figs. 3(a) to 3(d), respectively, where thick lines indicate the  $N$  profiles for  $P(H)$  and thin lines indicate the profiles for  $P(R)$ . The candidate embedding matrices are built in the same way as described in the Lorenz case study, that is,  $[P(H)_{(i)}, P(R)_{(i)}, P(H)_{(i+\tau)}]$  and  $[P(H)_{(i)}, P(R)_{(i)}, P(R)_{(i+\tau)}]$  are the candidate embedding matrices being tested for the first embedding cycle [Fig. 3(a)], and for the next embedding cycles, the candidate matrices are built based on the combination of variable and time delay selected in the previous cycle [Figs. 3(a) to 3(d), arrow]. As these are noisy profiles (see [3] for a comparison with profiles for  $L(X)$  contaminated with additive Gaussian white noise), the identi-

fication of local minima becomes more difficult and is sometimes balanced with the identification of a point at which a change in the decaying velocity of the profile occurs. From the second to the fourth embedding cycles [Figs. 3(b) to 3(d)], a peak is visible at previously selected  $\tau$  values, a feature also present in the noisy profiles reported in [3], which indicates that selecting the same  $\tau$  value would not only be a suboptimal choice, as it would indeed be the worst possible choice. Displayed in Fig. 3(e) is the fraction of F as a function of  $m$  [7], from which can be concluded that the optimal embedding dimension is  $m = 6$ , and the final embedding matrix is then  $[P(H)_{(i)}, P(R)_{(i)}, P(H)_{(i+\tau_1)}, P(H)_{(i+\tau_2)}, P(R)_{(i+\tau_3)}, P(R)_{(i+\tau_4)}]$ . The embedding of variables with different oscillatory frequencies, such as the heart rate  $P(H)$  and respiration  $P(R)$ , will initially be biased towards the variable with the higher frequency. This is clearly visible in Fig. 3(a), with  $P(H)$  presenting a substantially lower  $N$  profile than that of  $P(R)$ . However, this initial selection of  $P(H)$  is increasingly less advantageous, until the alternative variable  $P(R)$  is favored for the efficiency of the embedding.

The multivariate phase space reconstruction scheme could have been conceived in different ways, from embedding each variable separately and then adding them together, to the proposed iterative selection from an initial set of variables. The latter is more efficient, in the sense that the final embedding dimension is smaller than when variables are embedded separately. Such advantage is particularly relevant for massively multivariate systems, as for example proteomics or transcriptomic time series, which include hundreds or even thousands of variables [2]. Many of these variables will likely have a very strong correlation among themselves. In that case, the most efficient phase space reconstruction does not necessarily start with the concatenation of all variables without delay, as the approach suggested in this report. Instead, it should start with a single variable, to which additional variables, first without any delay, are then added. This small variation to the proposed algorithm addresses the issue of sufficient representation in multivariate systems with tight correlation between parameters. It is interesting to note that the proposed implementation in fact treats each variable as a surrogate for a delayed representation of the other variables. This is also particularly well suited for the representation of dynamic behavior documented by molecular biology time series for a very pragmatical reason - they tend to be very short, in the sense that the number of time points is typically many fold smaller than the number of variables.

The reverse engineering of biological processes from the time series they generate is often approached by parametrization of an explicit mathematical formulation [12]. It can be argued that this approach is hampered by the lack of exploratory tools that analyze the dynamic behavior directly to assist in selecting the most explanatory independent variables. Furthermore, the characteristic heterogeneity in oscillatory frequencies, large number of

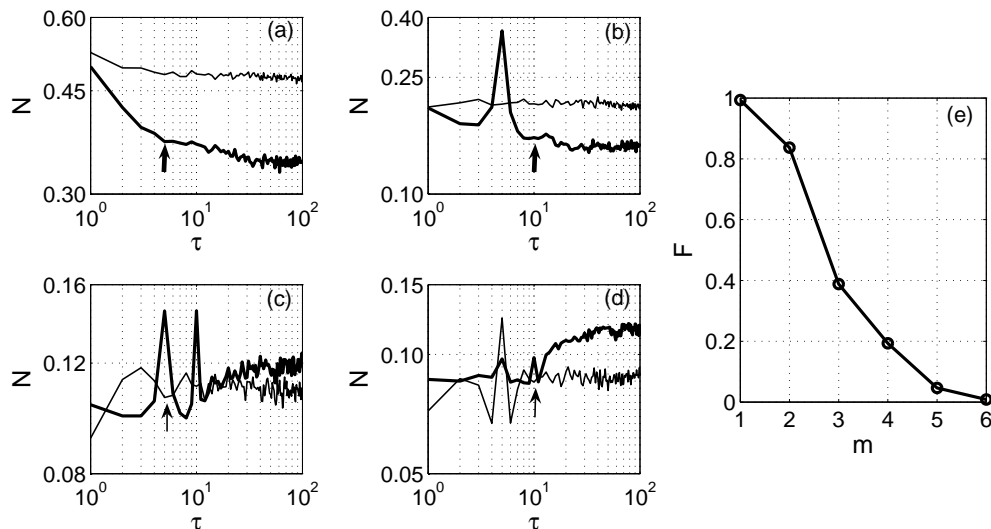


FIG. 3: (a) First, (b) second, (c) third and (d) fourth embedding cycle profiles for  $\tau$  selection from  $N$ . Thick lines indicate profiles for  $P(H)$  and thin lines indicate profiles for  $P(R)$ . An arrow indicates the optimal combination of variable and time delay selected from each embedding cycle. From the second (b) to the fourth (d) embedding cycles, a peak is visible at previously selected  $\tau$  values. (e) The fraction of  $F$  as a function of  $m$  for the embedding of the bivariate  $P(H)$  and  $P(R)$  time series. See the text for a more comprehensive description.

variables and short duration of the time series creates a particular challenge for approaching this exploratory analysis through the characterization of a reconstructed attractor. Accordingly, this report describes an attempt to use the criteria of efficient embedding to achieve that goal.

### Acknowledgments

Supported by Grants No. SFRH/BD/1165/2000 and No. POCTI/1999/BSE/34794 from Fundação para a

Ciência e a Tecnologia, Portugal, and by the National Heart, Lung and Blood Institute (NIH) Proteomics Initiative through Contract No. N01-HV-28181 (D. Knapp, PI).

- 
- [1] H.D.I. Abarbanel. *Analysis of Observed Chaotic Data*. Springer, New York, 1996.
- [2] M.Y. Galperin. *Nucl. Acids Res.*, 33:D5–D24, 2005.
- [3] S.P. Garcia and J.S. Almeida. Nearest neighbor embedding with different time delays. *Phys. Rev. E*, 71:037204, 2005.
- [4] R. Hegger, L. Jaeger, and H. Kantz. Reconstruction of the dynamics of noisy multivariate time series. Internal report, Max-Planck-Institut für Physik komplexer Systeme, 1997.
- [5] H. Kantz, J. Kurths, and G. Mayer-Kress (Eds.). *Nonlinear Analysis of Physiological Data*. Springer, Heidelberg, 1998.
- [6] H. Kantz and T. Schreiber. *Nonlinear Time Series Analysis*. Cambridge University Press, Cambridge, UK, 1997.
- [7] M.B. Kennel, R. Brown, and H.D.I. Abarbanel. *Phys. Rev. A*, 45:3403–3411, 1992.
- [8] E. Lorenz. *J. Atmos. Sci.*, 20:130–141, 1963.
- [9] D.R. Rigney, A.L. Goldberger, W.C. Ocasio, Y. Ichimaru, G.B. Moody, and R.G. Mark. *Time Series Prediction: Forecasting the Future and Understanding the Past*, volume Proc. Vol. XV of *SFI Studies in the Sciences of Complexity*, chapter Multi-channel physiological data: description and analysis (Data Set B), pages 105–129. Perseus Books, Reading, MA, 1st edition edition, 1994.
- [10] T. Sauer, J.A. Yorke, and M. Casdagli. *J. Stat. Phys.*, 65:579–616, 1991.
- [11] F. Takens. *Dynamical Systems and Turbulence*, volume 898 of *Lecture Notes in Mathematics*, pages 366–381. Springer-Verlag, Berlin, 1981.
- [12] E. Voit and J. Almeida. Decoupling dynamical systems for pathway identification from metabolic profiles. *Bioinformatics*, 20(11):1670–1681, 2004.